Empirical State-Space Representations
for Theodorsen's Lift Model

Steven L. Brunton, Clarence W. Rowley

Princeton University, Princeton, NJ 08544

Abstract

In this work, we cast Theodorsen's unsteady aerodynamic model into a general form that allows for the introduction of empirically determined quasi-steady and added-mass coefficients as well as an empirical Theodorsen function. An empirically determined Theodorsen model is constructed using data from direct numerical simulations of a flat plate airfoil pitching at low Reynolds number, Re = 100. Next, we develop low-dimensional, state-space realizations that are useful for either the classical Theodorsen lift model or the empirical model. The resulting model is parameterized by pitch-axis location and has physically meaningful states that isolate the effect of added-mass and quasi-steady forces, as well as the effect of the wake. A low-order approximation of Theodorsen's function is developed based on balanced truncation of a model fit to the analytical frequency response, and it is shown that this approximation outperforms other models from the literature. We demonstrate the utility of these state-space lift models by constructing a robust controller that tracks a reference lift coefficient by varying pitch angle while rejecting gust disturbances.

Keywords: Unsteady aerodynamics, Theodorsen's function, reduced order model, state-space realization

1. Introduction

Obtaining accurate and efficient aerodynamic models has been an important goal of research efforts in aeronautics over the past century. Aerodynamic models are necessary to design aircraft, to evaluate aeroelastic stability, and to develop feedback control laws. Among the wide range of unsteady aerodynamic models in the literature (Leishman, 2006), the classical models of Wagner (1925) and Theodorsen (1935) remain widely used and provide a benchmark for the linear models that proceed from them. Indeed, these models have been remarkably successful for over three-quarters of a century (Bisplinghoff and Ashley, 1962; Newman, 1977; Leishman, 2006). Garrick (1938) demonstrated the equivalence of Theodorsen's frequency-domain transfer function and Wagner's time-domain indicial response function.

There is a long and distinguished history of modeling various aspects of unsteady aerodynamics (Dowell et al., 1997; Dowell and Hall, 2001; Leishman, 2006). Theodorsen's model is particularly attractive, because it is derived from first principles using clear assumptions. The resulting model is broken down into physically meaningful components, including the added-mass and quasi-steady contributions as well as the effect of the wake, captured by Theodorsen's transfer function. It is then clear how the model changes as certain assumptions are relaxed. Additionally, the model is parameterized by the pitch center, x/c. Finally, the model is used extensively, which carries its own inherent value (Brar et al., 1996; Maitre et al., 2003; Bruno and Fransos, 2008).

Theodorsen's lift model was developed in 1935 to explain flutter induced instability that occurs in aircraft at high velocity. The theory is based on incompressible, inviscid assumptions, and the resulting model is expressed in the frequency domain. This limits the usefulness of this model, both for predicting the lift response in the time-domain, as well as for designing modern control laws. In addition, the inviscid assumption becomes less accurate for flows at low Reynolds number (Brunton and Rowley, 2009; Amiralaei et al., 2010), which are characterized by a thick, laminar boundary layer. Unsteady aerodynamics at low Reynolds number is of particular recent interest to understand insect and bird flight (Birch and Dickinson, 2001; Videler et al., 2004) as well as to develop advanced controllers for high performance micro-aerial vehicles (Zbikowski, 2002; Eldredge et al., 2009; OL, 2010; Kerstens et al., 2011).

We address both of these limitations in this paper. First, we develop an empirical generalization to Theodorsen's model, extending the model to various geometries and Reynolds numbers. In particular, empirical models from simulations or experiments are cast into the form of Theodorsen's model using empirical added-mass and quasi-steady lift coefficients, as well as an empirical Theodorsen function. The method of obtaining an empirical Theodorsen model is demonstrated for a flat plate pitching at low Reynolds number, Re = 100.

Next, state-space representations are developed for either the classical Theodorsen lift model or the empirical lift model. These state-space models are desirable because they fit naturally into existing flight models, and they are useful for the design of optimal controllers (Dullerud and Paganini, 2000; Skogestad and Postlethwaite, 2005). The models are constructed to isolate the effect of added-mass and quasi-steady forces, as well as the effect of the wake, as in Theodorsen's original model. In addition, the models maintain the original pitch-axis parameterization. It is important to note that although Theodorsen's model includes the effect of an aileron and also describes moment calculations, we consider only the lift coefficient output for pitch and plunge motion.

1.1. Previous work on representations of Theodorsen's model

The literature contains a number of rational function approximations to Theodorsen's transfer function, given in Eq. (3) below, such as those presented in R.T. Jones (1938), Vepa (1977), Venkatesan and Friedmann (1986), and Breuker et al. (2008). There are also approximations to Wagner's indicial response function, derived in Garrick (1938), R.T. Jones (1938), W.P. Jones (1945), and Venkatesan and Friedmann (1986), many of which are based on Padé approximation. Dowell (1980) demonstrated a method for converting frequency-domain models to the time domain. Dinyavari and Friedmann (1986) and Breuker et al. (2008) constructed state-space realizations for Theodorsen's transfer function, and Leishman and Nguyen (1990) used R. T. Jones's approximation for the indicial response function to derive a state-space realization for the circulatory lift. Edwards et al. (1978) derived a state-space realization for the coupled aeroelastic equations, which he used to construct a linear-quadratic-regulator for flutter suppression.

Peters et al. (2007) and Peters (2008) developed a general potential flow theory in state-space based on the Glauert expansion of inflow states, of which Theodorsen's model is a special case. However, Peters's model requires eight states for close agreement with Theodorsen's model, while the other approximations require between two and four states. With the exception of Peters, none of the above references develop state-space models for the full unsteady model (Eq. (2) below), including added-mass forces.

In this paper, we develop a state-space representation for Theodorsen's full unsteady lift model that retains the physically motivated properties of the original model; this includes pitch-axis parameterization and separation of added-mass, quasi-steady, and wake effects. The state-space modeling framework is sufficiently general that any of the above approximations for Theodorsen's function may be used. In addition, it is shown how an empirical Theodorsen function may be obtained for a specific geometry and Reynolds number, allowing the inviscid assumption to be relaxed. We also present a new state-space approximation of Theodorsen's function, based on balanced truncation, that is more accurate than those in the literature.

2. Background

Wagner (1925) developed a model for the unsteady lift on a two-dimensional airfoil for arbitrary pitching motion. He computed analytically the effect of idealized planar wake vorticity on the circulation around the airfoil

in response to a step in angle of attack. After this, the response to arbitrary motion could be constructed by convolution with this indicial response. Ten years later, Theodorsen (1935) derived a related model to study the aeroelastic problem of flutter instability. Wagner's and Theodorsen's theories are derived analytically for an idealized two-dimensional flat plate airfoil moving through an inviscid, incompressible fluid. The motion of the flat plate is assumed to be infinitesimal, leaving an idealized planar wake. Both theories refine the quasi-steady theory (Eq. (1) below) by including the effect of the wake history on the induced circulation around the airfoil. Section 2.3 demonstrates the equivalence of Theodorsen's transfer function and Wagner's indicial response function via Laplace transform (Garrick, 1938; Jones, 1938). Additional derivation and review of Theodorsen's theory may be found in Bisplinghoff and Ashley (1962), Leishman (2006), and Newman (1977).

2.1. Theodorsen's Model

Theodorsen's model is an unsteady extension of the quasi-steady thin airfoil theory to include added-mass forces and the effect of wake vorticity. Thin airfoil theory assumes that the vertical center of mass h and angle of attack α motion of the airfoil is relatively slow and small, so that the flow field locally equilibrates to the motion. Thus, the effects of $\dot{h}$ and $\dot{\alpha}$ appear as an effective angle of attack and an effective camber, respectively, which may be combined into a total effective angle of attack for the entire airfoil. This results in a quasi-steady expression for the lift coefficient:

$$C_L^{\mathrm{QS}} = 2\pi \left(\alpha + \dot{h} + \dot{\alpha} \left(\frac{1}{2} - a \right) \right) = 2\pi \alpha_e \tag{1}$$

where a is the pitch axis location measured in semi-chords with respect to the mid-chord (e.g., pitching about the leading edge corresponds to $a = -1$, whereas the trailing edge is $a = 1$). Lengths are nondimensionalized by the half-chord length, b, and velocity is nondimensionalized by the free-stream velocity, U_∞, so that time is nondimensionalized by the half-chord convection time, b/U_∞.

For rapid maneuvers, it is necessary to include added-mass terms to account for the reaction force due to the mass of fluid that is accelerated by the airfoil. Additionally, one must account for the induced circulation around the airfoil due to the wake vorticity. Theodorsen's model includes these added-mass forces and multiplies the quasi-steady lift from thin airfoil theory by a transfer function $C(k)$ to account for lift attenuation by the wake vorticity:

$$C_L = \underbrace{\pi \left[\ddot{h} + \dot{\alpha} - a\ddot{\alpha} \right]}_{\text{Added-Mass}} + \underbrace{2\pi \left[\alpha + \dot{h} + \dot{\alpha} \left(\frac{1}{2} - a \right) \right]}_{\text{Quasi-steady}} C(k). \tag{2}$$

Theodorsen's transfer function $C(k)$ is expressed in terms of Hankel functions $H_\nu^{(2)} = J_\nu - iY_\nu$, where J_ν and Y_ν are Bessel functions of the first and second kind, respectively, and is given by

$$C(k) = \frac{H_1^{(2)}(k)}{H_1^{(2)}(k) + iH_0^{(2)}(k)}. \tag{3}$$

This expression is well-defined only for purely sinusoidal airfoil motion with a reduced frequency $k = \omega b/U_\infty$. Edwards (1977) derived a generalized Theodorsen's function, $C(\bar{s})$, in terms of modified Bessel functions of the second kind, $K_\nu(\bar{s})$, which is defined on the entire complex plane. $\bar{s} = sb/U_\infty$ is a dimensionless Laplace variable. When $\bar{s} = ik$, $C(\bar{s})$ returns the classical Theodorsen function for a sinusoidal input with reduced frequency k.

Figure 1 shows the frequency response of Theodorsen's model, Eq. (2). The input motion is $\ddot{h}$ for the case of plunging and $\ddot{\alpha}$ for the case of pitching, and the output is lift coefficient C_L. Theodorsen's model for pitching motion is parameterized by $a = -1 + 2x/c$, where x/c is the pitch axis location measured in positive chord lengths c from the leading edge.

It is helpful to gain a physical intuition for the frequency response (i.e., Bode plot) and how it relates to the aerodynamic response. The magnitude plot (top) shows the ratio of output magnitude (C_L) to input magnitude ($\ddot{\alpha}$ or $\ddot{h}$) in decibels (dB) for sinusoidal forcing at various fixed frequencies, and the phase plot (bottom) shows the corresponding phase difference in degrees. The low-frequency asymptote in the Bode magnitude plot corresponds to the quasi-steady case when the lift coefficient depends only on the angle of attack in the case of pitch, or effective angle of attack in the case of plunge. For pitching motion, the low-frequency asymptote has a slope of -40 dB/decade, consistent with the fact that α is obtained by integrating the input $\ddot{\alpha}$ twice. In the case of plunge, the low-frequency asymptote has a slope of -20 dB/decade, since the effective angle of attack is proportional to $\dot{h}$ which is the integral of the input $\ddot{h}$.

The high-frequency asymptote in the Bode magnitude plot corresponds to the case where there are large accelerations and the lift coefficient is strongly influenced by added-mass forces. In the case of pitching with $a > 0$
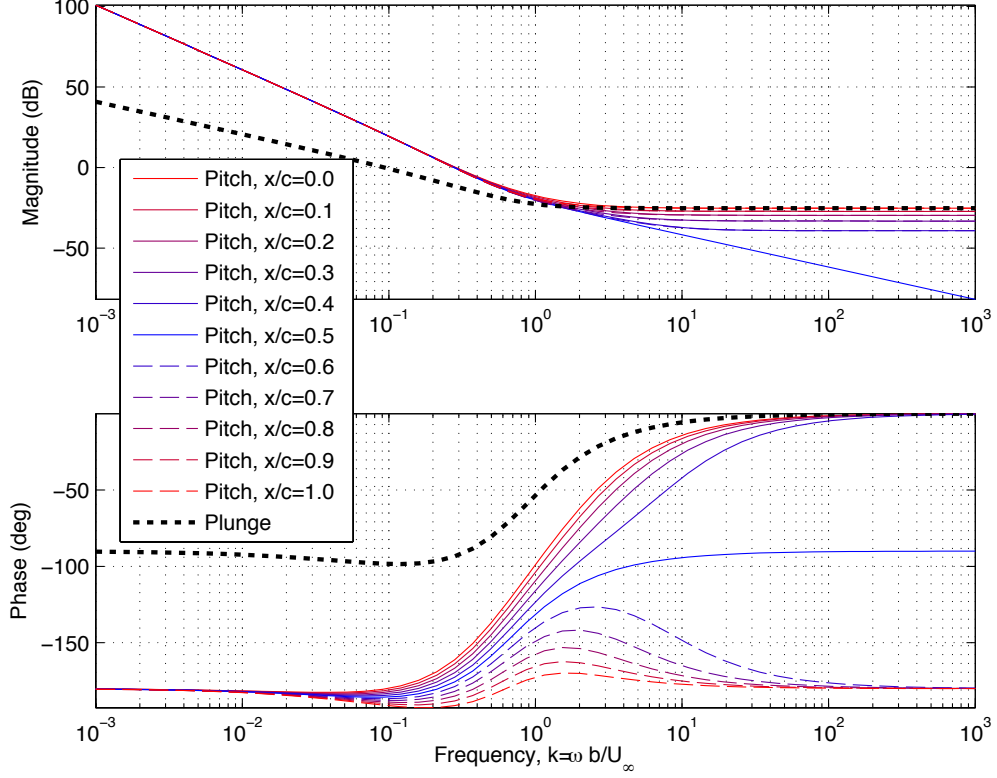
Figure 1: Frequency response of Theodorsen's model, Eq. (2). Input is $\ddot{h}$ for plunging motion and $\ddot{\alpha}$ for pitching motion about various locations x/c along the chord. The output is lift coefficient C_L.

and plunge motion, there are added-mass forces directly proportional to the inputs ($\ddot{\alpha}$ and $\ddot{h}$), so that the Bode plot has zero slope at high frequencies. There are no added-mass forces proportional to $\ddot{\alpha}$ in the case of mid-chord pitching, but there are forces proportional to $\dot{\alpha}$, so the Bode plot has a slope of -20 dB/decade at high frequencies. This information is also reflected in the Bode phase plot. Notice that the phase at low frequency starts at $-180°$ for the pitching models, which is consistent with the fact that the angle of attack is the second integral of the input; twice integrating a sinusoid results in another negative sinusoid, hence the $-180°$ phase.

The frequency response in Figure 1 undergoes a qualitative change as the pitch point is moved aft of the mid-chord. At this point, the effect of added-mass terms on high frequency motions becomes negative; i.e., the phase approaches $-180°$ for large frequency. A direct result is that given a positive step in angle of attack, the lift initially moves in the negative direction, because of negative added-mass forces, before the circulatory forces have a chance to catch up and the system relaxes to a positive steady state.

2.2. Wagner's model

Wagner's model is similar to Theodorsen's, except that it is formulated in the time domain, making it useful for arbitrary input maneuvers. The model rests on a similar assumptions, including a planar wake, inviscid, incompressible flow, and infinitesimal motion. The formulation is based on convolution with the (indicial) step response function, $\phi(\tau)$, where $\tau = tU_\infty/b$ is time nondimensionalized by the half-chord convection time. At time $\tau = 0$ the aerodynamic center is located at the mid-chord, and it shifts to the quarter-chord, $x/c = 0.25$, for all future time, $\tau > 0$. The lift due to the step is:

$$C_L^\delta = \pi\delta(\tau) + 2\pi\alpha\phi(\tau) \tag{4}$$

The first term is the added-mass for a step in angle of attack about the mid-chord. The circulatory terms for an arbitrary maneuver $\alpha(\tau)$ are given by

$$C_L^{\text{circ}} = 2\pi\left(\alpha(0)\phi(\tau) + \int_0^\tau \dot{\alpha}(\sigma)\phi(\tau - \sigma)\,d\sigma\right) = 2\pi\alpha_e(\tau) \tag{5}$$

where $\alpha_e(\tau)$ is the effective angle of attack due to the induced circulation from the wake history.
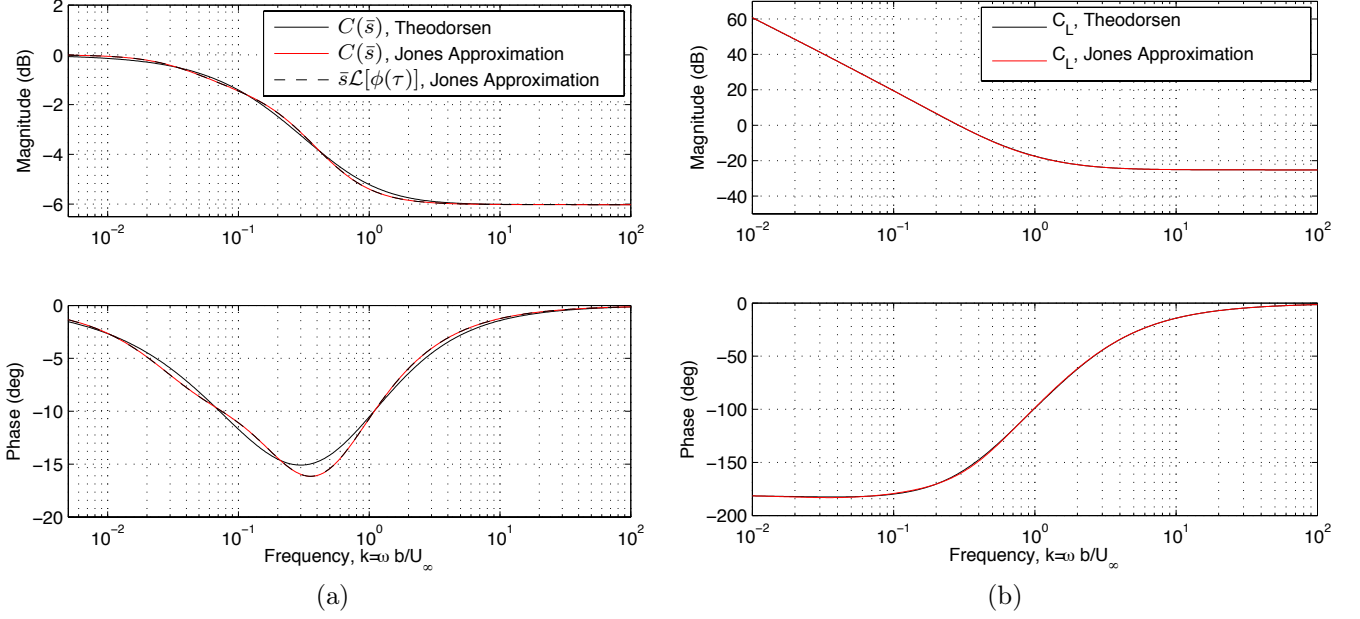
4

Figure 2: (a) Frequency response of Theodorsen's transfer function $C(\bar{s})$ (black) and the R.T. Jones approximation for $C(\bar{s})$ (red) and $\bar{s}\mathcal{L}[\phi(\tau)]$ (black dash), respectively. (b) Frequency response for full lift model.

2.3. Relationship between Wagner's and Theodorsen's functions, $\phi(\tau)$ and $C(\bar{s})$

Garrick (1938) and Jones (1938) observed that Theodorsen's transfer function, $C(\bar{s})$, and Wagner's indicial response function, $\phi(\tau)$, are related by a Laplace transform pair:

$$C(\bar{s}) = \bar{s} \int_0^\infty \phi(\tau) e^{-\bar{s}\tau} \, d\tau \qquad (6)$$

Therefore, Theodorsen's and Wagner's functions are equivalent representations of the effect of the wake in the frequency domain and time domain, respectively. There are a number of rational function approximations to Theodorsen's transfer function $C(\bar{s})$ in the literature, compiled in the second column of Table 1, and to Wagner's indicial response function $\phi(\tau)$, compiled in the second column of Table 3, in Section 4.4. Figure 2 shows a frequency response comparison between the exact Theodorsen function in Eq. (2) and the R.T. Jones approximation for $C(\bar{s})$ and $\phi(\tau)$ from Tables 1 and 3. These will be useful in Section 4 for obtaining state-space realizations.

3. Generalized Theodorsen model

It is possible to generalize Theodorsen's model by replacing the coefficients π and 2π, that are obtained using linearized potential flow theory, with generalized coefficients C_1 and C_2. The new coefficients may be obtained empirically, either through simulation or experiment, for a given Reynolds number and wing geometry. This will yield better performance in the limit of low and high frequency motions. Additionally, it is possible to determine an empirical function $\hat{C}(\bar{s})$ that plays the same role as Theodorsen's $C(\bar{s})$. Eq. (2) becomes:

$$C_L = C_1 \left[\ddot{h} + \dot{\alpha} - a\ddot{\alpha} \right] + C_2 \left[\alpha + \dot{h} + \dot{\alpha} \left(\frac{1}{2} - a \right) \right] \hat{C}(\bar{s}). \qquad (7)$$

We now take the Laplace transform, $\mathcal{L}$, of both sides to obtain a transfer function. For the case of pitch, $u = \ddot{\alpha}$,

$$\frac{\mathcal{L}[C_L]}{\mathcal{L}[\ddot{\alpha}]} = C_1 \left(\frac{1}{\bar{s}} - a \right) + C_2 \left[\frac{1}{\bar{s}^2} + \frac{1}{\bar{s}} \left(\frac{1}{2} - a \right) \right] \hat{C}(\bar{s}) \qquad (8)$$

where $\bar{s}$ is the dimensionless Laplace variable. The transfer function $1/\bar{s}$ corresponds to integration in the time domain. Equation (8) is represented schematically in Figure 3.

The case of plunging, $u = \ddot{h}$, has a simpler transfer function:

$$\frac{\mathcal{L}[C_L]}{\mathcal{L}[\ddot{h}]} = C_1 + \frac{C_2}{\bar{s}} \hat{C}(\bar{s})$$

These transfer functions will be used to construct state-space representations in the next section.
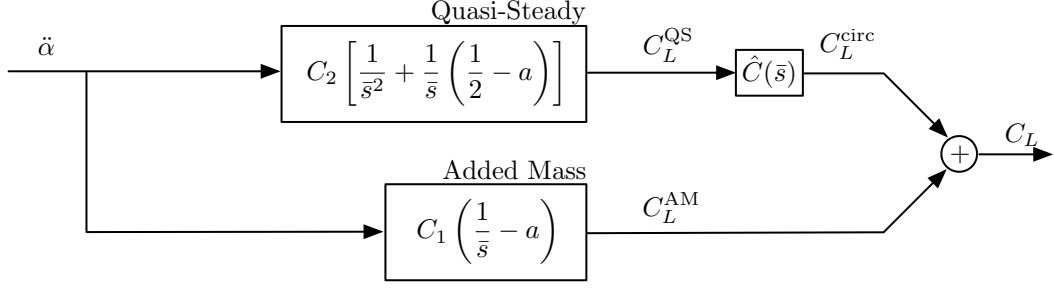
5

Figure 3: Empirical Theodorsen's model, Eq. (8), for a pitching airfoil.

3.1. Determining coefficients C_1 and C_2

Theodorsen's function is 1 at low frequencies and $1/2$ at high frequencies. Decomposing it as $C(\bar{s}) = 1 - C'(\bar{s})$ results in the following pitch model:

$$C_L = \underbrace{-aC_1}_{C_{\ddot{\alpha}}} \ddot{\alpha} + \underbrace{\left[C_1 + C_2 \left(\frac{1}{2} - a\right)\right]}_{C_{\dot{\alpha}}} \dot{\alpha} + \underbrace{C_2}_{C_{\alpha}} \alpha - \underbrace{C_2 C'(\bar{s}) \left[\alpha + \dot{\alpha}\left(\frac{1}{2} - a\right)\right]}_{\text{transient dynamics}} \tag{9}$$

Equation (9) yields expressions for the coefficients in terms of stability derivatives, $C_1 = -C_{\ddot{\alpha}}/a$ and $C_2 = C_{\alpha}$, which may be determined empirically. There are a number of ways to model the additional transient dynamics. The simplest approach is to use the analytic Theodorsen function $C(\bar{s})$; in this case, the empirically determined C_1 and C_2 still guarantee the correct high and low frequency behavior. For better performance at intermediate frequencies, it is possible to determine an empirical Theodorsen function $\hat{C}(\bar{s})$, as discussed in the next section.

3.2. Empirical Theodorsen function $\hat{C}(\bar{s})$

Starting with an accurate state-space model for a given Reynolds number and geometry, it is possible to determine an empirical Theodorsen function, $\hat{C}(\bar{s})$. Starting with a transfer function model, $G(\bar{s})$, from $\ddot{\alpha}$ to C_L, it is possible to solve for $\hat{C}(\bar{s})$ in Eq. (8) by first subtracting off the added-mass terms and then dividing through by the quasi-steady terms:

$$\hat{C}(\bar{s}) = \frac{G(\bar{s}) - C_1\left(1/\bar{s} - a\right)}{C_2\left[1/\bar{s}^2 + (1/2 - a)/\bar{s}\right]} \tag{10}$$

The empirical Theodorsen function $\hat{C}(\bar{s})$ is demonstrated in Figure 4 (a) for a model of a plate pitching about the leading-edge at Re = 100. The empirical model has order $r = 2$; the resulting lift coefficient model is shown in Figure 4 (b).

4. State-space realizations for Theodorsen's lift model

Starting with Theodorsen's model, Eq. (2), or the empirical model, Eq. (8), we construct a state-space representation of the form:

$$\begin{aligned}\dot{x} &= Ax + Bu \\ y &= Cx + Du\end{aligned} \qquad \Longleftrightarrow \qquad \left[\begin{array}{c}\dot{x} \\ y\end{array}\right] = \left[\begin{array}{c|c}A & B \\ \hline C & D\end{array}\right]\left[\begin{array}{c}x \\ u\end{array}\right] \tag{11}$$

$u \in \mathbb{R}^q$ is the input, $y \in \mathbb{R}^p$ is the output, and $x \in \mathbb{R}^n$ is the state; the matrix notation is shorthand. These representations are carefully constructed to retain the favorable properties of Theodorsen's original model. In particular, the model is parameterized by the pitch-axis location, and the added-mass and quasi-steady forces are isolated from the effect of the wake. Moreover, the states of the model are physically meaningful quantities.

Consider state-space realizations for the quasi-steady (QS) and Theodorsen transfer function blocks in Figure 3:

$$\text{Quasi-steady:} \qquad \begin{aligned}\dot{x}' &= A'x' + B'u' \\ y' &= C'x'\end{aligned} \tag{12}$$

$$\text{Theodorsen:} \qquad \begin{aligned}\dot{\tilde{x}} &= \tilde{A}\tilde{x} + \tilde{B}\tilde{u} \\ \tilde{y} &= \tilde{C}\tilde{x} + \tilde{D}\tilde{u}\end{aligned} \tag{13}$$
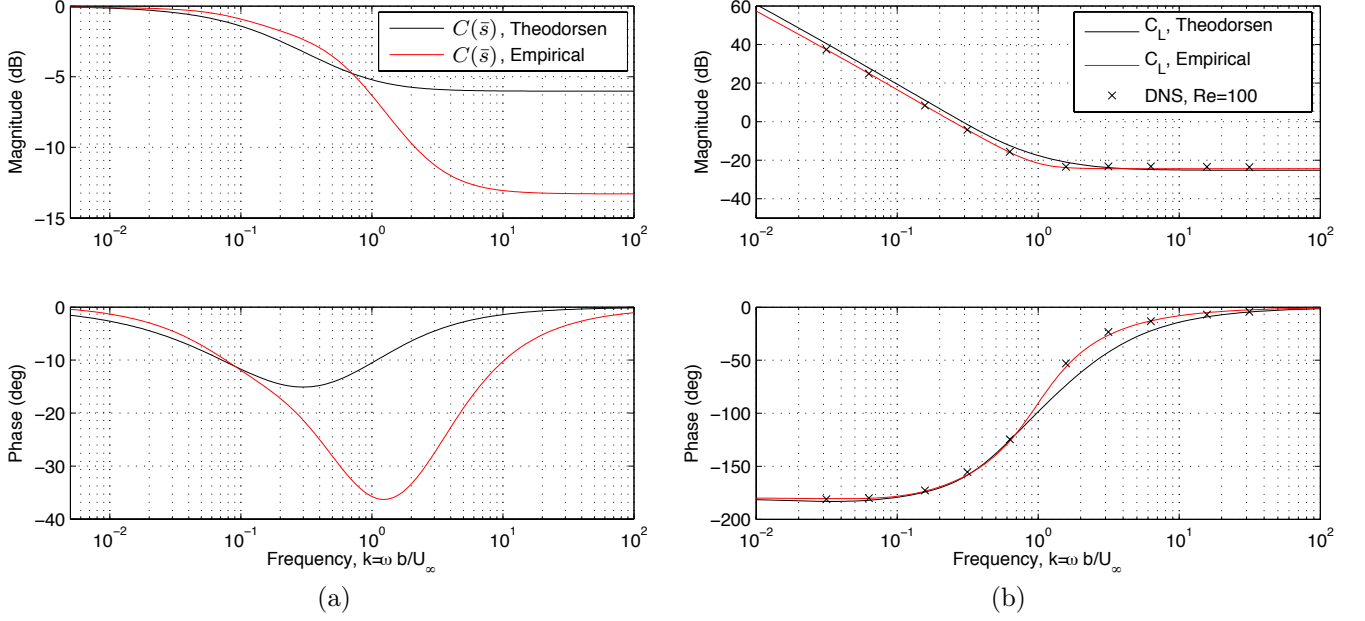
6

Figure 4: (a) Frequency response of Theodorsen's transfer function, $C(\bar{s})$, from theory (black) and empirical $\hat{C}(\bar{s})$ for a flat plate pitching about the leading edge, $x/c = 0.0$, at Re $= 100$ (red). (b) Frequency response of full lift model. Direct numerical simulations ($\times$) are included for comparison.

The output of the quasi-steady model is the input to Theodorsen's transfer function, $y' = \tilde{u}$, resulting in:

$$\frac{d}{dt}\begin{bmatrix} \tilde{x} \\ x' \end{bmatrix} = \begin{bmatrix} \tilde{A} & \tilde{B}C' \\ 0 & A' \end{bmatrix}\begin{bmatrix} \tilde{x} \\ x' \end{bmatrix} + \begin{bmatrix} 0 \\ B' \end{bmatrix} u'$$

$$\tilde{y} = \begin{bmatrix} \tilde{C} & \tilde{D}C' \end{bmatrix}\begin{bmatrix} \tilde{x} \\ x' \end{bmatrix} \qquad \Longleftrightarrow \qquad \left[\begin{array}{cc|c} \tilde{A} & \tilde{B}C' & 0 \\ 0 & A' & B' \\ \hline \tilde{C} & \tilde{D}C' & 0 \end{array}\right] \qquad (14)$$

State-space realizations $(\tilde{A}, \tilde{B}, \tilde{C}, \tilde{D})$ for Theodorsen's function will be presented in Section 4.4.

4.1. Pure pitch model

For the case of pure pitching motion, $u = \ddot{\alpha}$, the quasi-steady transfer function from Eq. (8) is given by

$$\text{QS}(\bar{s}) = C_2\left[\bar{s}^{-2} + \bar{s}^{-1}(1 - 2a)/2\right] \qquad (15)$$

To obtain a realization for Eq. (15), we introduce the state $x' = \begin{bmatrix} \alpha & \dot{\alpha} \end{bmatrix}^T$, input $u' = \ddot{\alpha}$, and output $y' = C_L^{\text{QS}}$:

$$\frac{d}{dt}\begin{bmatrix} \alpha \\ \dot{\alpha} \end{bmatrix} = \begin{bmatrix} 0 & 1 \\ 0 & 0 \end{bmatrix}\begin{bmatrix} \alpha \\ \dot{\alpha} \end{bmatrix} + \begin{bmatrix} 0 \\ 1 \end{bmatrix}\ddot{\alpha}$$

$$C_L^{\text{QS}} = \begin{bmatrix} C_2 & C_2\left(1 - 2a\right)/2 \end{bmatrix}\begin{bmatrix} \alpha \\ \dot{\alpha} \end{bmatrix} \qquad (16)$$

The quasi-steady lift coefficient, C_L^{QS}, depends on α and $\dot{\alpha}$, which comprise the state, x'. The added-mass transfer function is $\text{AM}(\bar{s}) = C_1\left[\bar{s}^{-1} - a\right]$. With state $x = \dot{\alpha}$, input $u = \ddot{\alpha}$, and output $y = C_L^{\text{AM}}$, a state-space realization for the added-mass portion is:

$$\frac{d}{dt}\dot{\alpha} = \ddot{\alpha}$$

$$C_L^{\text{AM}} = C_1\dot{\alpha} - C_1 a\ddot{\alpha} \qquad (17)$$

7

The quasi-steady and added-mass models share a state $\dot{\alpha}$, so we may represent the total lift in a compact model:

$$\frac{d}{dt}\begin{bmatrix}\tilde{x}\\\alpha\\\dot{\alpha}\end{bmatrix}=\begin{bmatrix}\tilde{A}&\tilde{B}C_2&\tilde{B}C_2\left(1-2a\right)/2\\0&0&1\\0&0&0\end{bmatrix}\begin{bmatrix}\tilde{x}\\\alpha\\\dot{\alpha}\end{bmatrix}+\begin{bmatrix}0\\0\\1\end{bmatrix}\ddot{\alpha}$$

(18)

$$C_L=\begin{bmatrix}\tilde{C}&\tilde{D}C_2&C_1+\tilde{D}C_2\left(1-2a\right)/2\end{bmatrix}\begin{bmatrix}\tilde{x}\\\alpha\\\dot{\alpha}\end{bmatrix}-C_1a\ddot{\alpha}$$

In this model, we have combined the quasi-steady model in Eq. (16) with the model of Theodorsen's function in Eq. (13) according to the formula in Eq. (14), and we have included the additional added-mass forces from Eq. (17).

4.2. Pure plunge model

For plunge, $u=\ddot{h}$, the quasi-steady transfer function is $\text{QS}(\bar{s})=C_2\bar{s}^{-1}$ and the added-mass force is $C_1\ddot{h}$. This results in the following combined model

$$\frac{d}{dt}\begin{bmatrix}\tilde{x}\\\dot{h}\end{bmatrix}=\begin{bmatrix}\tilde{A}&\tilde{B}C_2\\0&0\end{bmatrix}\begin{bmatrix}\tilde{x}\\\dot{h}\end{bmatrix}+\begin{bmatrix}0\\1\end{bmatrix}\ddot{h}$$

(19)

$$C_L=\begin{bmatrix}\tilde{C}&\tilde{D}C_2\end{bmatrix}\begin{bmatrix}\tilde{x}\\\dot{h}\end{bmatrix}+C_1\ddot{h}$$

Note that there is no dependence of lift on the vertical height, h, only on its derivatives.

4.3. Combined pitch and plunge model

For combined pitch and plunge, $u=\begin{bmatrix}\ddot{h}&\ddot{\alpha}\end{bmatrix}^T$, the model is given by:

$$\frac{d}{dt}\begin{bmatrix}\tilde{x}\\\dot{h}\\\alpha\\\dot{\alpha}\end{bmatrix}=\begin{bmatrix}\tilde{A}&\tilde{B}C_2&\tilde{B}C_2&\tilde{B}C_2(1-2a)/2\\0&0&0&0\\0&0&0&1\\0&0&0&0\end{bmatrix}\begin{bmatrix}\tilde{x}\\\dot{h}\\\alpha\\\dot{\alpha}\end{bmatrix}+\begin{bmatrix}0&0\\1&0\\0&0\\0&1\end{bmatrix}\begin{bmatrix}\ddot{h}\\\ddot{\alpha}\end{bmatrix}$$

(20)

$$C_L=\begin{bmatrix}\tilde{C}&\tilde{D}C_2&\tilde{D}C_2&C_1+\tilde{D}C_2(1-2a)/2\end{bmatrix}\begin{bmatrix}\tilde{x}\\\dot{h}\\\alpha\\\dot{\alpha}\end{bmatrix}+\begin{bmatrix}C_1&-C_1a\end{bmatrix}\begin{bmatrix}\ddot{h}\\\ddot{\alpha}\end{bmatrix}$$

This realization is not minimal, since the state $\begin{bmatrix}0&1&-1&0\end{bmatrix}^T$ is unobservable. This is consistent with the fact that in Theodorsen's framework, $\dot{h}$ contributes to an effective angle of attack after proper nondimensionalization. It is possible to construct a minimal realization by introducing the state variable $\alpha_e=\alpha+\dot{h}$, resulting in:

$$\frac{d}{dt}\begin{bmatrix}\tilde{x}\\\alpha_e\\\dot{\alpha}\end{bmatrix}=\begin{bmatrix}\tilde{A}&\tilde{B}C_2&\tilde{B}C_2(1-2a)/2\\0&0&1\\0&0&0\end{bmatrix}\begin{bmatrix}\tilde{x}\\\alpha_e\\\dot{\alpha}\end{bmatrix}+\begin{bmatrix}0&0\\1&0\\0&1\end{bmatrix}\begin{bmatrix}\ddot{h}\\\ddot{\alpha}\end{bmatrix}$$

(21)

$$C_L=\begin{bmatrix}\tilde{C}&\tilde{D}C_2&C_1+\tilde{D}C_2(1-2a)/2\end{bmatrix}\begin{bmatrix}\tilde{x}\\\alpha_e\\\dot{\alpha}\end{bmatrix}+\begin{bmatrix}C_1&-C_1a\end{bmatrix}\begin{bmatrix}\ddot{h}\\\ddot{\alpha}\end{bmatrix}$$

This representation is more compact because the pitch and plunge models share the same dynamics, $\tilde{A}$.

	Approximate transfer function, $C_r(\bar{s})$	$\left[\begin{array}{c|c} \tilde{A} & \tilde{B} \\ \hline \tilde{C} & \tilde{D} \end{array}\right]$, State-space realization of $C_r(\bar{s})$
R.T. Jones (1938)	$\dfrac{0.5\bar{s}^2 + 0.2808\bar{s} + 0.01365}{\bar{s}^2 + 0.3455\bar{s} + 0.01365}$	$\left[\begin{array}{cc|c} -0.3455 & -0.01365 & 1 \\ 1 & 0 & 0 \\ \hline 0.1081 & .006825 & 0.5 \end{array}\right]$
Vepa (1977)	$\dfrac{\bar{s}^4 + 0.761\bar{s}^3 + 0.1021\bar{s}^2 + 2.551e^{-3}\bar{s} + 9.557e^{-6}}{2\bar{s}^4 + 1.064\bar{s}^3 + 0.1134\bar{s}^2 + 2.617e^{-3}\bar{s} + 9.557e^{-6}}$	$\left[\begin{array}{cccc|c} -0.532 & -0.0567 & -0.001308 & -4.779e^{-6} & 1 \\ 1 & 0 & 0 & 0 & 0 \\ 0 & 1 & 0 & 0 & 0 \\ 0 & 0 & 1 & 0 & 0 \\ \hline 0.1145 & 0.0227 & 6.212e^{-4} & 2.389e^{-6} & 0.5 \end{array}\right]$
Venkatesan & Friedman (1986)	$\dfrac{0.5(\bar{s} + 0.088)(\bar{s} + 0.37)(\bar{s} + 0.922)}{(\bar{s} + 0.072)(\bar{s} + 0.261)(\bar{s} + 0.80)}$	$\left[\begin{array}{ccc|c} -1.133 & -0.2852 & -0.01503 & 1 \\ 1 & 0 & 0 & 0 \\ 0 & 1 & 0 & 0 \\ \hline 0.1235 & 0.08482 & 0.007493 & 0.5 \end{array}\right]$
Breuker et al. (2008)	$\dfrac{0.5177\bar{s}^2 + 0.2752\bar{s} + 0.01576}{\bar{s}^2 + 0.3414\bar{s} + 0.01582}$	$\left[\begin{array}{cc|c} -0.3414 & -0.01582 & 1 \\ 1 & 0 & 0 \\ \hline 0.09846 & 0.00757 & 0.5177 \end{array}\right]$
Balanced truncation	$\dfrac{0.5\bar{s}^4 + 0.703\bar{s}^3 + 0.2393\bar{s}^2 + 0.01894\bar{s} + 2.318e^{-4}}{\bar{s}^4 + 1.158\bar{s}^3 + 0.3052\bar{s}^2 + 0.02028\bar{s} + 2.325e^{-4}}$	$\left[\begin{array}{cccc|c} -1.158 & -0.3052 & -0.02028 & -2.325e^{-4} & 1 \\ 1 & 0 & 0 & 0 & 0 \\ 0 & 1 & 0 & 0 & 0 \\ 0 & 0 & 1 & 0 & 0 \\ \hline 0.124 & 0.08667 & 0.008805 & 1.156e^{-4} & 0.5 \end{array}\right]$

Table 1: Rational function approximations, $C_r(\bar{s})$, to Theodorsen's transfer function, $C(\bar{s})$, and state-space representations.

		Existing models			Balanced Truncation		
	R.T. Jones	Breuker et al.	Venkatesan & Friedman	Vepa	$r = 4$	$r = 5$	$r = 6$
$\|C - C_r\|_\infty$ (dB)	-36.73	-35.04	-33.81	-43.16	-50.62	-57.32	-62.14

Table 2: Norm of error, $\|C - C_r\|_\infty$, between various models, C_r, and Theodorsen's exact function, C, in decibels (dB).

4.4. State-space realizations for Theodorsen's function $C(\bar{s})$ and Wagner's function $\phi(\tau)$

To obtain the $\tilde{A}, \tilde{B}, \tilde{C}$, and $\tilde{D}$ in Eq. (13), there are a number of rational approximations to Theodorsen's function $C(\bar{s})$, Eq. (3), including the approximations of Jones (1938), Vepa (1977), Venkatesan and Friedmann (1986) and Breuker et al. (2008). For each of these transfer functions it is possible to obtain a state-space realization in controller canonical form. Both the transfer function and state-space realization are presented in Table 1 for each approximation. The resulting lift model, using Jones's approximation, agrees well with the exact Theodorsen model, as shown in Figure 2 (b). Figure 5 shows the magnitude of the error in each approximation.

We also develop a new state-space approximation for Theodorsen's transfer function $C(\bar{s})$. Using the analytic expression in Eq. (3), we compute the values of Theodorsen's function at 1200 points logarithmically spaced in the interval $[10^{-3}, 10^2]$. These data points are then used to construct a stable, minimum phase, 11th-order state-space realization using the Matlab function, `fitfrd`. Finally, balanced truncation is applied to obtain a reduced order model, C_r, of order r. The balanced model of order $r = 4$ is presented in Table 1. The comparison of these balanced truncation models with different order of truncation is also shown in Figure 5 and Table 2. For order $r \geq 4$, the balanced truncation models have smaller error norm, $\|C - C_r\|_\infty$, than previous models from the literature. It is also possible to obtain reduced order models using the method of balanced residualization, which yields exact agreement at low frequencies, but these models typically have larger error at moderate and high frequencies.

It is also possible to obtain state-space realizations for Wagner's indicial response, $\phi(\tau)$. Realizations based on R.T. Jones's approximation (1938) have been previously developed by Dinyavari and Friedmann (1986) and by Leishman and Nguyen (1990). The Laplace transform of the indicial response function ϕ is the transfer function from $\dot{\alpha}$ to the circulatory lift coefficient C_L^{circ}. Garrick's approximation from Table 3 is a simple expression, but it does not have a simple Laplace transform. The other two expressions in Table 3 have the form $\phi(\tau) = 1 - a_1 e^{-b_1\tau} - a_2 e^{-b_2\tau}$.
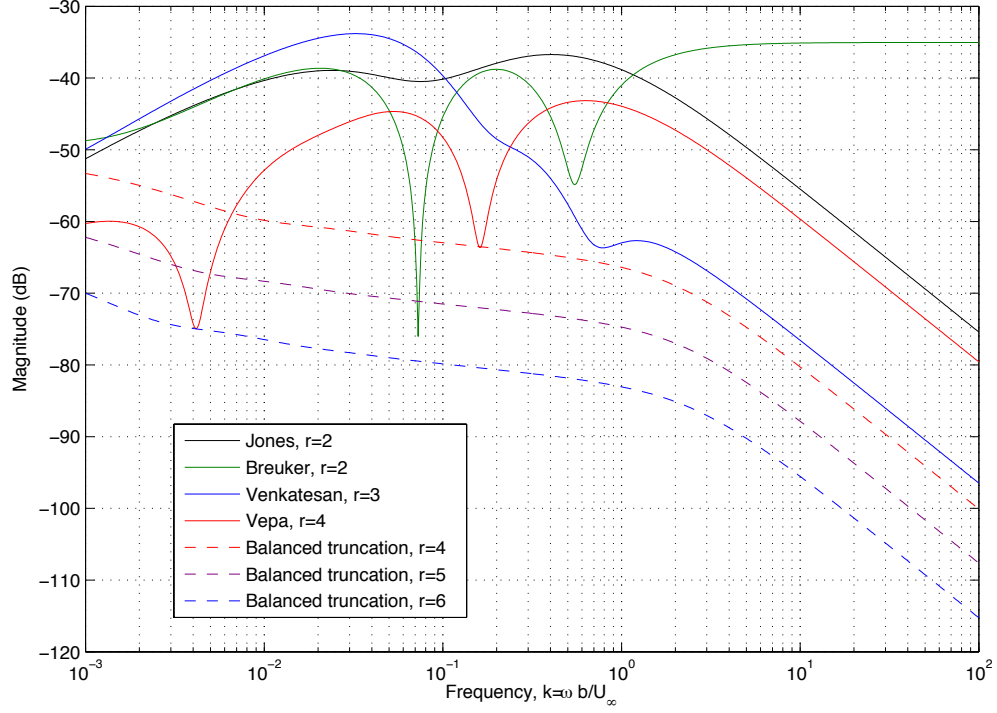
Figure 5: Magnitude of error between exact Theodorsen's function, $C(\bar{s})$, and various reduced-order models, $C_r(\bar{s})$.

	Approximate indicial response, $\phi(\tau)$	$\left[\begin{array}{c\|c}\tilde{A} & \tilde{B} \\ \hline \tilde{C} & \tilde{D}\end{array}\right]$, State-space realization of $\phi(\tau)$
Garrick (1938)	$\dfrac{\tau + 2}{\tau + 4}$	Not a rational expression
R.T. Jones (1938)	$1.0 - 0.165e^{-0.0455\tau} - 0.335e^{-0.3\tau}$	$\left[\begin{array}{ccc\|c} -0.3455 & -0.01365 & 0 & 1 \\ 1 & 0 & 0 & 0 \\ 0 & 1 & 0 & 0 \\ \hline 0.5 & 0.2808 & 0.01365 & 0 \end{array}\right]$
W.P. Jones (1945)	$1.0 - 0.165e^{-0.041\tau} - 0.335e^{-0.32\tau}$	$\left[\begin{array}{ccc\|c} -0.361 & -0.01312 & 0 & 1 \\ 1 & 0 & 0 & 0 \\ 0 & 1 & 0 & 0 \\ \hline 0.5 & 0.2945 & 0.01312 & 0 \end{array}\right]$
Venkatesan & Friedman (1986)	$1.0 - 0.203e^{-0.072\tau} - 0.236e^{-0.261\tau} - 0.06e^{-0.8\tau}$	$\left[\begin{array}{cccc\|c} -1.133 & -0.2852 & -0.01503 & 0 & 1 \\ 1 & 0 & 0 & 0 & 0 \\ 0 & 1 & 0 & 0 & 0 \\ 0 & 0 & 1 & 0 & 0 \\ \hline 0.501 & 0.6918 & 0.2281 & 0.01503 & 0 \end{array}\right]$

Table 3: Approximations for Wagner's indicial response function $\phi(\tau)$.

The Laplace transform of $\phi(\tau)$ is:

$$\mathcal{L}\phi(\tau) = \frac{1}{\bar{s}} - \frac{a_1}{\bar{s} + b_1} - \frac{a_2}{\bar{s} + b_2} \tag{22}$$

This yields the state-space realizations with input $\dot{\alpha}$ and output C_L^{circ} in Table 3.

Because of the equivalence of Wagner's function $\phi(\tau)$ and Theodorsen's transfer function $C(\bar{s})$, it is not necessary to develop an explicit state-space realization for Wagner's full unsteady model.
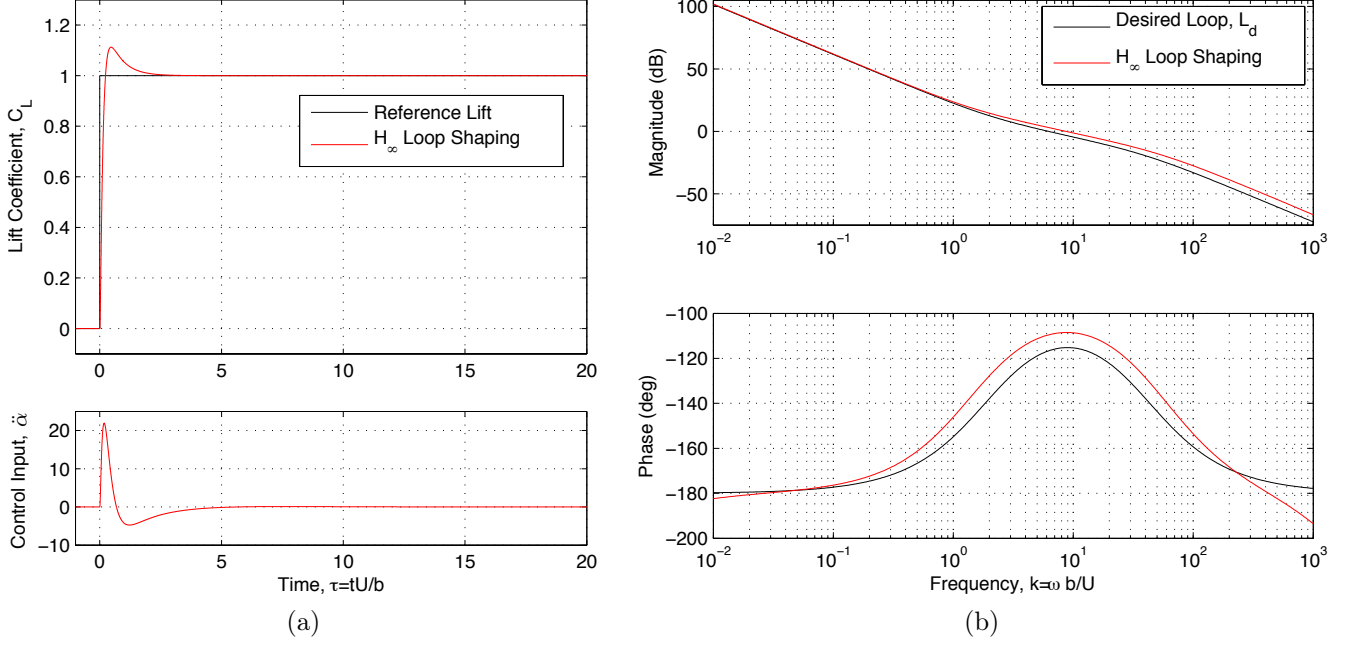
Figure 6: (a) Controller performance on a step maneuver. (b) Bode plot of loop transfer function.

5. Robust lift control based on Theodorsen's model

The pitch model derived in Section 4.1 is now used to develop a robust controller to track a reference lift, r, by varying the pitch angle. The system is now given by

$$\begin{aligned}\dot{x} &= Ax + Bu \\ y &= Cx + Du,\end{aligned} \tag{23}$$

where (A, B, C, D) is a state-space representation of Theodorsen's lift model, given by Eq. (18). The output is a lift measurement, $y = C_L$, and the input is pitch acceleration, $u = \ddot{\alpha}$. The controller input is $y - r$, the error signal.

We now design a robust controller using $\mathcal{H}_\infty$ loop-shaping design. In this control design method, one chooses a desired loop transfer function, $L = GK$, where $G(\bar{s}) = C(\bar{s}I - A)^{-1}B + D$ is the transfer function for the unsteady aerodynamic system, and K is the controller. We choose the desired loop gain to be

$$L_d = \frac{240(\bar{s} + 2)}{\bar{s}^2(\bar{s} + 40)}, \tag{24}$$

shown in Figure 6 (b). This loop transfer function is a double integrator (as is the aerodynamic system G, at low frequencies), adjusted to have a slope of about 1 near the crossover frequency, which we choose to be $10 \, \mathrm{rad/s}\, b/U$. Given this desired loop transfer function, $\mathcal{H}_\infty$ loop-shaping provides a robust controller K. As shown in Figure 6 (b), the resulting loop gain $L = GK$ is close to the desired shape, L_d, but with a larger phase margin at crossover. We include an actuator model, $G_a = 250/(\bar{s} + 250)$, in the loop to impose actuator roll-off at high frequency, since the plant has a non-zero D matrix.

Figure 6 (a) shows the performance of the controller in response to a unit step in the commanded lift coefficient at time $\tau = 0$. Figure 7 demonstrates the controller for an aggressive reference tracking scenario with the addition of a disturbance, d, and sensor noise, n. Both d and n are stochastic processes; we assume that they are uncorrelated zero-mean white-noise Gaussian processes with variance $W = 1.0$ and $V = 10^{-4}$, respectively. The reference lift signal is a sequence of pseudo-random ramp-hold maneuvers. The middle plot shows the noisy error signal, $y - r + n$ that is sent to the controller, along with the true error, $\Delta C_L = C_L - r$. The bottom plot shows the control signal, $\ddot{\alpha}$. Note that the error remains small throughout the maneuver, and the measurement noise is attenuated by the controller.

6. Summary

In this paper, a generalized Theodorsen model is developed and cast into a low-dimensional, state-space representation. Using a number of rational function approximations for Theodorsen's transfer function $C(\bar{s})$ from Jones
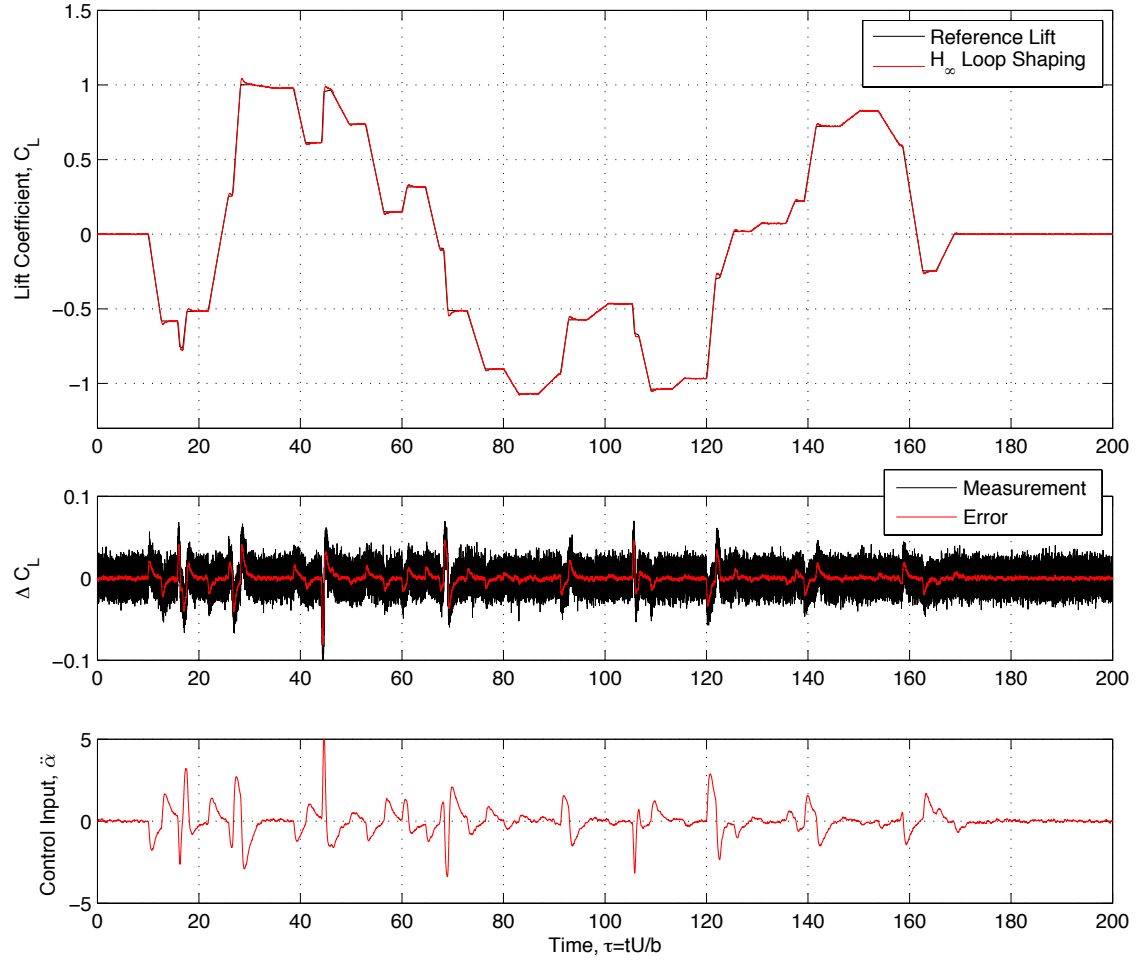
Figure 7: Controller performance on an aggressive maneuver. (top) Lift coefficient during maneuver. (middle) Noisy measurement, $C_L - r + n$, and tracking error, $C_L - r$. (bottom) Control input

(1938), Vepa (1977), Venkatesan and Friedmann (1986), and Breuker et al. (2008), we obtain a corresponding minimal state-space representation for Theodorsen's lift model, given by Eq. (18) for pure pitch, Eq. (19) for pure plunge, and Eq. (21) for combined pitch and plunge. We also develop a new approximation for Theodorsen's transfer function based on balanced truncation of a frequency-response data model. The state-space lift models retain the positive attributes of Theodorsen's model, in that they are parameterized by pitch axis and have physically meaningful states that isolate the effect of quasi-steady and added-mass forces, as well as the effect of the wake. A state-space realization for Wagner's indicial response function $\phi(\tau)$ is also included. However, because of the equivalence of Wagner's function, $\phi(\tau)$, with Theodorsen's function, $C(\bar{s})$, via Laplace transform, we have focused on developing state-space representations of Theodorsen's model.

Additionally, a method is presented to obtain empirical added-mass and quasi-steady coefficients, C_1 and C_2, as well as an empirical Theodorsen function, $\hat{C}(\bar{s})$, using either simulations or experiments. Correct coefficients C_1 and C_2 guarantee agreement of the model in the limit of high and low frequency motions, and the function $\hat{C}(\bar{s})$ ensures agreement at intermediate frequencies. An empirically determined Theodorsen's model has been demonstrated for a flat plate pitching at low Reynolds number, Re = 100.

Finally, a robust controller is developed based on the state-space form of Theodorsen's model for a pitching airfoil, Eq. (18). The resulting controller tracks a reference lift by varying the angle of attack while rejecting gust disturbances and attenuating measurement noise. The use of modern control techniques, such as $\mathcal{H}_2$ and $\mathcal{H}_\infty$ optimal control, and $\mathcal{H}_\infty$ loop shaping, is a key motivation for developing these state-space representations for Theodorsen's model.

There are a number of interesting avenues for future research. Further investigation of the empirical Theodorsen function, $\hat{C}(\bar{s})$, for various wing geometry and Reynolds numbers may provide insight into the fundamental unsteady boundary layer physics at low Reynolds number. It will also be interesting to develop optimal controllers for combined pitch and plunge motion for use in flight control. Finally, the state-space models developed here will

provide a framework for incorporating additional unsteady phenomena, such as dynamic stall.

Acknowledgements

References

Amiralaei, M. R., Alighanbari, H., Hashemi, S. M., 2010. An investigation into the effects of unsteady parameters on the aerodynamics of a low Reynolds number pitching airfoil. Journal of Fluids and Structures 26, 979–993.

Birch, J., Dickinson, M., 2001. Spanwise flow and the attachment of the leading-edge vortex on insect wings. Nature 412, 729–733.

Bisplinghoff, R. L., Ashley, H., 1962. Principles of Aeroelasticity. John Wiley & Sons, Inc., Hoboken, New Jersey.

Brar, P. S., Raul, R., Scanlan, R. H., 1996. Numerical calculation of flutter derivatives via indicial functions. Journal of Fluids and Structures 10, 337–351.

Breuker, R. D., Abdalla, M., Milanese, A., Marzocca, P., April 2008. Optimal control of aeroelastic systems using synthetic jet actuators. AIAA Paper 2008-1726, 49th Structures, Structural Dynamics, and Materials Conference.

Bruno, L., Fransos, D., 2008. Evaluation of Reynolds number effects on flutter derivatives of a flat plate by means of a computational approach. Journal of Fluids and Structures 24, 1058–1076.

Brunton, S. L., Rowley, C. W., January 2009. Modeling the unsteady aerodynamic forces on small-scale wings. AIAA Paper 2009-1127, 47th Aerospace Sciences Meeting.

Dinyavari, M. A. H., Friedmann, P. P., 1986. Application of time-domain unsteady aerodynamics to rotary-wing aeroelasticity. AIAA Journal 24 (9), 1424–1432.

Dowell, E. H., 1980. A simple method for converting frequency-domain aerodynamics to the time domain. Technical Memorandum 81844, NASA.

Dowell, E. H., Hall, K. C., 2001. Modeling of fluid-structure interaction. Annual Review of Fluid Mechanics 33, 445–490.

Dowell, E. H., Hall, K. C., Romanowski, M. C., 1997. Eigenmode analysis in unsteady aerodynamics: Reduced-order models. Applied Mechanics Reviews 50 (6), 371–386.

Dullerud, G. E., Paganini, F., 2000. A course in robust control theory: A convex approach. Texts in Applied Mathematics. Springer, Berlin, Heidelberg.

Edwards, J. W., 1977. Unsteady aerodynamic modeling and active aeroelastic control. SUDARR 504, Stanford University.

Edwards, J. W., Breakwell, J. V., Jr., A. E. B., 1978. Active flutter control using generalized unsteady aerodynamic theory. Journal of Guidance and Control 1, 32–40.

Eldredge, J. D., Wang, C., OL, M. V., June 2009. A computational study of a canonical pitch-up, pitch-down wing maneuver. AIAA Paper 2009-3687, 39th Fluid Dynamics Conference.

Garrick, I. E., 1938. On some reciprocal relations in the theory of nonstationary flows. Tech. Rep. 629, NACA.

Jones, R. T., 1938. Operational treatment of the non-uniform lift theory in airplane dynamics. Technical Note 667, NASA.

Jones, W. P., 1945. Aerodynamic forces on wings in nonuniform motion. R & M 2117, ARC.

Kerstens, W., Pfeiffer, J., Williams, D., King, R., Colonius, T., 2011. Closed-loop control of lift for longitudinal gust suppression at low Reynolds numbers. AIAA Journal 49 (8), 1721–1728.

Leishman, J. G., 2006. Principles of Helicopter Aerodynamics, 2nd Edition. Cambridge University Press, Cambridge, England.

Leishman, J. G., Nguyen, K. Q., 1990. A state-space representation of unsteady aerodynamic behavior. AIAA Journal 28 (5), 836–845.

Maitre, O. P. L., Scanlan, R. H., Knio, O. M., 2003. Estimation of the flutter derivative of an NACA airfoil by means of Navier-Stokes simulation. Journal of Fluids and Structures 17, 1–28.

Newman, J., 1977. Marine Hydrodynamics. The MIT Press, Cambridge, Massachusetts.

OL, M. V., 2010. Unsteady low Reynolds number aerodynamics for micro air vehicles (MAVs). Technical Report 2010-3013, Air Force Research Laboratory.

Peters, D. A., 2008. Two-dimensional incompressible unsteady airfoil theory– an overview. Journal of Fluids and Structures 24, 295–312.

Peters, D. A., Hsieh, M. A., Torrero, A., 2007. A state-space airloads theory for flexible airfoils. Journal of the American Helicopter Society 52, 329–342.

Skogestad, S., Postlethwaite, I., 2005. Multivariable feedback control: analysis and design, 2nd Edition. John Wiley & Sons, Inc., Hoboken, New Jersey.

Theodorsen, T., 1935. General theory of aerodynamic instability and the mechanism of flutter. Tech. Rep. 496, NACA.

Venkatesan, C., Friedmann, P. P., 1986. A new approach to finite state modelling of unsteady aerodynamics. AIAA Journal 24 (12), 1889–1897.

Vepa, R., 1977. Finite state modeling of aeroelastic systems. Contractor Report 2779, NASA.

Videler, J. J., Samhuis, E. J., Povel, G. D. E., 2004. Leading-edge vortex lifts swifts. Science 306, 1960–1962.

Wagner, H., 1925. Über die Entstehung des dynamischen Auftriebes von Tragflügeln. Zeitschrift für Angewandte Mathematic und Mechanik 5 (1), 17–35.

Zbikowski, R., 2002. On aerodynamic modelling of an insect-like flapping wing in hover for micro air vehicles. Philosophical Transactions of the Royal Society A 360, 273–290.